JOURNAL OF CATALYSIS **81**, 382–393 (1983)

Encapsulation: A New Mechanism of Catalyst Deactivation

BOB R. POWELL AND SHELL E. WHITTINGTON

Physical Chemistry Department, General Motors Research Laboratories, Warren, Michigan 48090

Received October 7, 1982

Silica-supported platinum model catalysts show evidence of encapsulation when annealed at 1200 and 1375 K. The 100-nm Pt particles become partially immersed in the SiO_2 surface with concurrent formation of an SiO_2 ridge around the base of the Pt particles. A model of these processes has been developed which predicts this behavior based on the reduction of the surface free energy of the Pt/SiO_2 system. Partial Pt encapsulation at lower temperatures and in more highly dispersed Pt catalysts is discussed and is shown to be a possible and as yet unreported mechanism of deactivation.

INTRODUCTION

One important process by which supported platinum catalysts deactivate is particle growth. This form of deactivation is due to the decrease in the percentage of exposed Pt atoms that occurs with increasing particle size. The mechanisms of particle growth are (1) particle migration and coalescence (*1, 2*), and (2) interparticle diffusion or ripening (*3*). One factor that influences the mechanisms of Pt particle growth is the support. On alumina, Pt particles larger than 2.5 nm are immobile, so that particle growth occurs by interparticle diffusion (*4*). Smaller Pt particles appear to migrate and coalesce into larger particles (*1*). When supported on silica, 1-nm Pt particles grow by interparticle diffusion of Pt atoms or PtO_2 molecules (*5*).

We have identified a new process by which the area of exposed Pt surface is reduced. This process, encapsulation, converts exposed Pt surface area into Pt-support interfacial area. This decrease in the surface area to interfacial area ratio occurs when hemispherical Pt particles on the SiO_2 surface change shape to a lenticular configuration in which the Pt particle is partially encapsulated in the SiO_2 support. The driving force of encapsulation is the reduction of the free energy of the Pt/SiO_2 system.

In this paper we (1) present experimental evidence for Pt encapsulation on SiO_2 supports, (2) identify and model the thermodynamic driving force of encapsulation, and (3) discuss the implications of encapsulation for the particle growth mechanisms of migration and ripening.

EXPERIMENTAL METHODS

The samples used in this study were thin film model catalysts. Pt was sputter deposited as a thin film onto flat, 0.3-cm-diameter disks of fused SiO_2. The SiO_2 disks were cleaned prior to Pt deposition by sequential immersion in ultrasonic baths of acetone, 1,1,1-trichloroethane, and methanol. After air drying, the disks were placed in the vacuum chamber of the sputtering system and evacuated to 0.1 mPa.

The Pt was RF sputtered in 99.999% argon at 4.4 Pa. The sputtering unit was a simple diode system, Perkin–Elmer Randex Model 2400. Seven seconds of sputtering at 400 W and 2100 V produced a Pt film approximately 8 nm thick. The thickness was determined by depth profiling techniques in which the Pt Auger electron intensity was monitored during argon ion milling through the film. The as-deposited film was continuous, but could be broken up into discrete particles by annealing. Annealing

0021-9517/83 $3.00

conditions ranged from 4 h at 975 K to 0.5 h at 1200 K.

The Pt/SiO_2 samples were examined using a scanning electron microscope (SEM). To reduce charging under electron bombardment, a 20-nm film of carbon was evaporated onto each sample before inserting it into the microscope.

RESULTS AND DISCUSSION

The evolution of the microstructure of a Pt/SiO_2 thin film model catalyst is shown in Fig. 1. The as deposited 8-nm-thick Pt film, shown in Fig. 1a, is continuous and reveals the flatness of the SiO_2 surface. If the Pt film is thermodynamically unstable, a thermal treatment should cause the film to collapse into a lower energy configuration. Since the free energies of the Pt surface (*6*) and presumably the Pt–SiO_2 interface (*7*) are greater than the free energy of the SiO_2 surface (*8*), a lower energy configuration would consist of discrete Pt particles and exposed SiO_2 surface. Annealing in air for 4 h at 975 K (Fig. 1b) caused a partial collapse of the Pt film into discrete particles, while further annealing in air for 0.5 h at 1200 K completed the process (Fig. 1c). The result is a distribution of nearly round Pt particles on the flat SiO_2 surface.

The microstructure shown in Fig. 1d was produced by annealing the sample in air for 24 h at 1200 K. The SiO_2 surface appears to have bulged, forming a ridge around the Pt particles. In some locations the ridge occurred but Pt particles were not observed, suggesting that a Pt particle that was originally circumscribed by the ridge had been removed. Microstructural features can also be seen in Fig. 2 which is a stereograph of a Pt/SiO_2 sample which was annealed for 10 days at 1375 K in a sealed, evacuated SiO_2 capsule. The stereograph shows Pt particles which are nearly hemispherical while the SiO_2 surface at the base of these particles has deformed and is covering part of the Pt surface. As before, empty depressions circumscribed by ridges are evident. Figure 3 is a stereograph of the same sample taken at a lower magnification, showing that these phenomena appear consistently over the sample.

The initial effect of annealing, i.e., the breakup of the Pt film, is analogous to the preparation of a catalyst in the sense that annealing produces dispersed Pt particles on the SiO_2 surface. We use the term encapsulation to describe the subsequent effect of annealing which was observed in Figs. 1d, 2, and 3. We believe encapsulation includes (1) SiO_2 growth around the Pt particles, and (2) Pt immersion into the SiO_2 surface. We also believe that encapsulation of Pt on SiO_2 is a thermodynamically driven process that, like particle growth, lowers the area of exposed Pt surface and is consequently a mechanism of thermal deactivation of catalysts. We have constructed a model of encapsulation as a thermodynamic process. We will (1) describe the thermodynamic model of the encapsulation process, (2) discuss the assumptions necessary to apply the model, and (3) discuss encapsulation as a mechanism of catalyst deactivation and its implications for theories of particle growth.

The Model

We define the initial state of our thermodynamic system to be one hemispherical Pt particle supported on a planar SiO_2 surface (Fig. 4). The free energy of this system is

$$F = \sigma_{\mathrm{Pt}}A_{\mathrm{Pt}} + \sigma_{\mathrm{SiO_2}}A_{\mathrm{SiO_2}} + \sigma_{\mathrm{int}}A_{\mathrm{int}}, \quad (1)$$

where σ is the surface energy and A is the area of the surface or interface. Pt, SiO_2, and int refer to the Pt surface, the SiO_2 surface, and the Pt–SiO_2 interface, respectively. Defined this way, F is the free energy of the Pt/SiO_2 system due only to the presence of surfaces and interfaces. F does not include internal energy or energy arising from curvature of the surfaces or interfaces, i.e., the Kelvin equation. The effect of curvature as well as the reasonableness of other assumptions of the model will be discussed later. Pt and SiO_2 are assumed to be in chemical equilibrium with

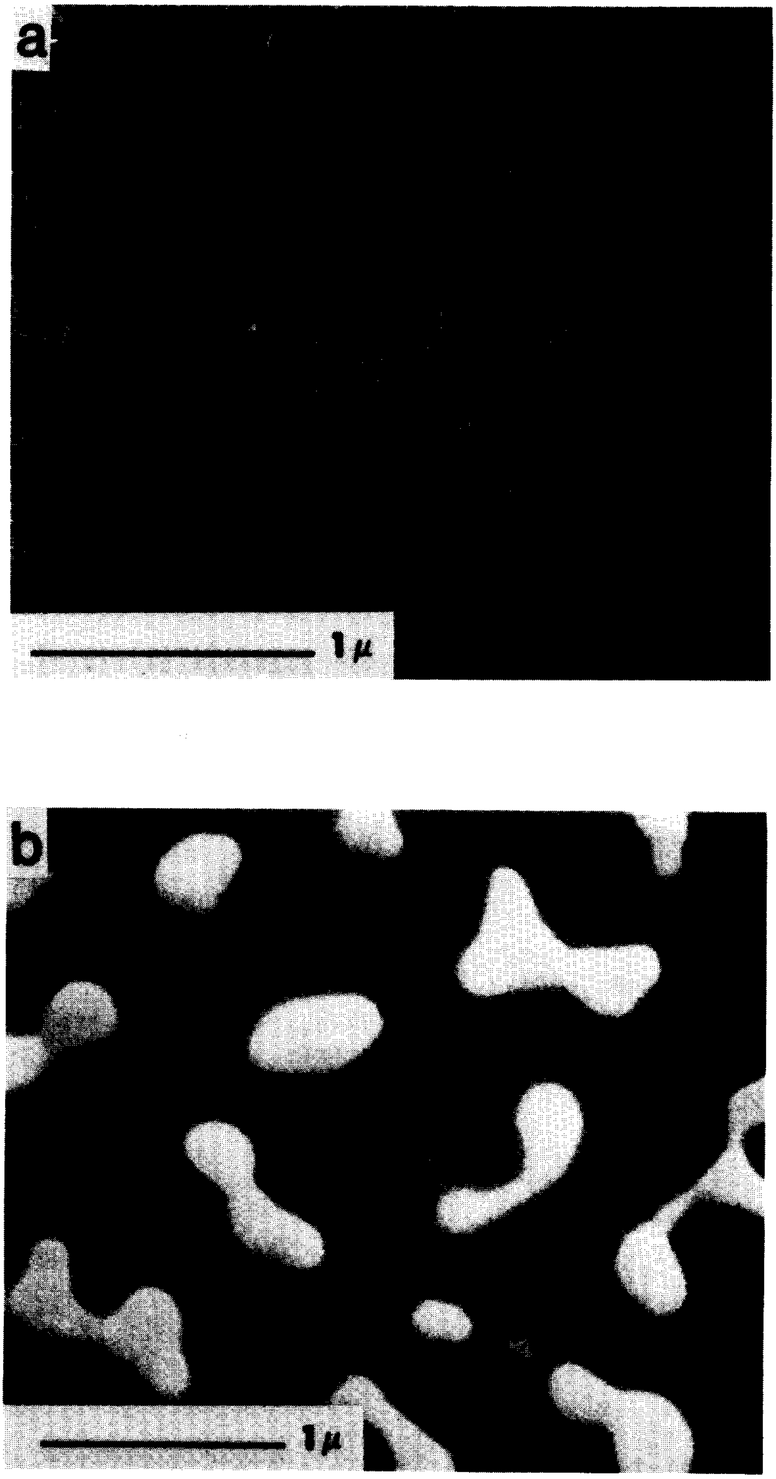

FIG. 1. The effect of annealing on the microstructure of Pt particles supported on SiO_2. SEM results for (a) as deposited, (b) annealed in air (4 h, 975 K), (c) further annealed in air (0.5 h, 1200 K), and (d) further annealed in air (24 h, 1200 K).

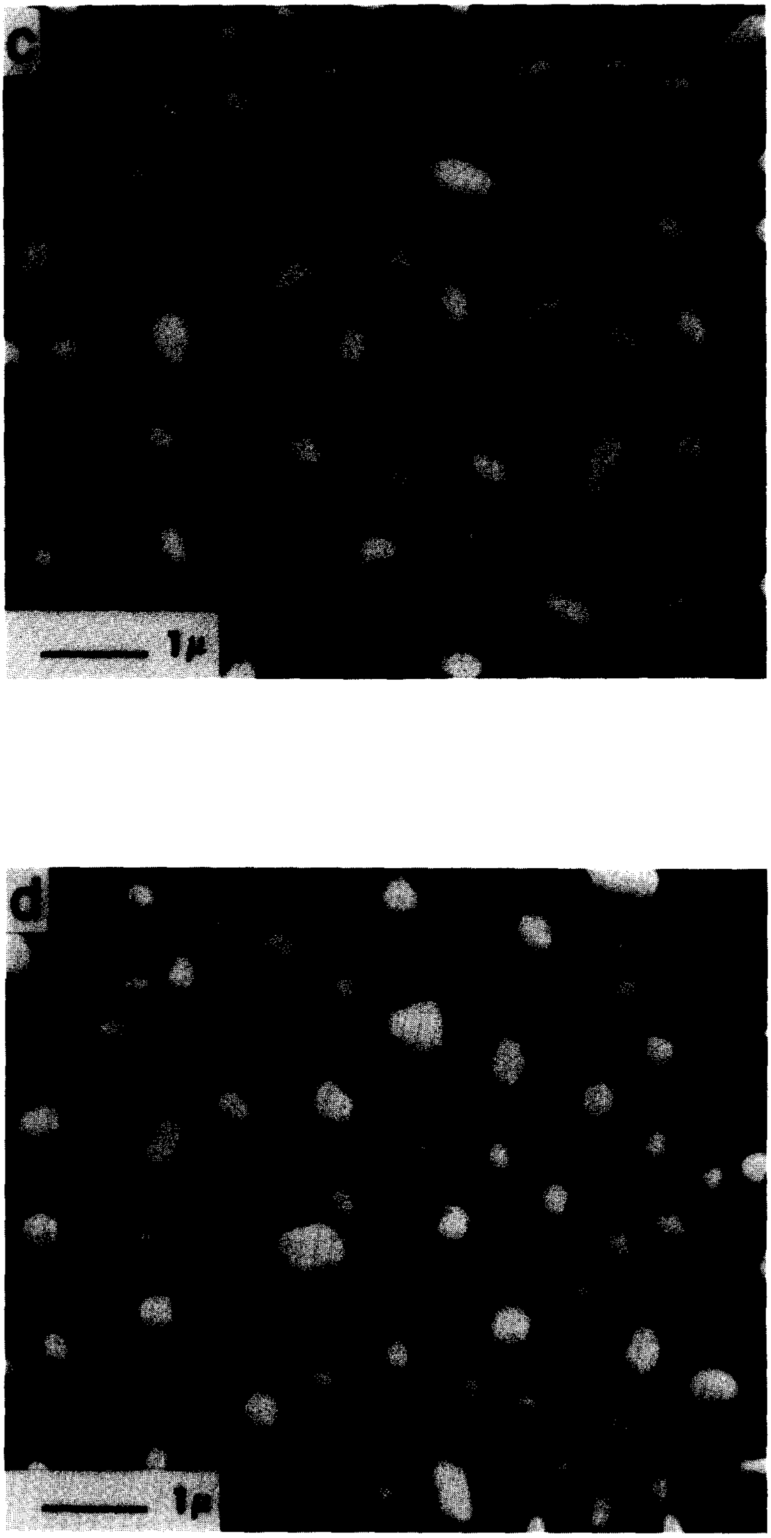

FIG. 1—*Continued.*

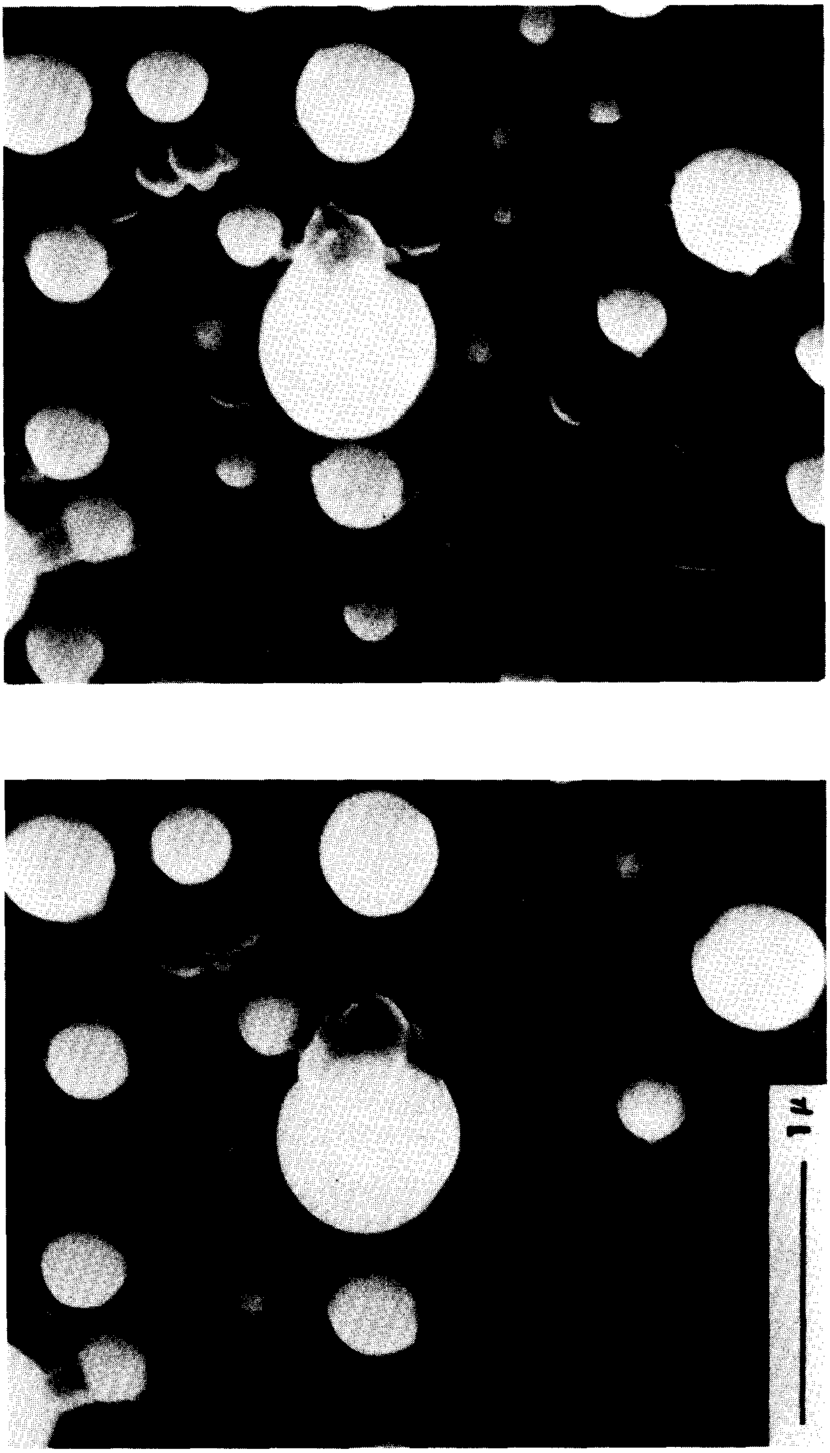

FIG. 2. SEM stereograph of air-annealed Pt/SiO$_2$ model catalyst (10 days, 1375 K, 5.3 Pa).

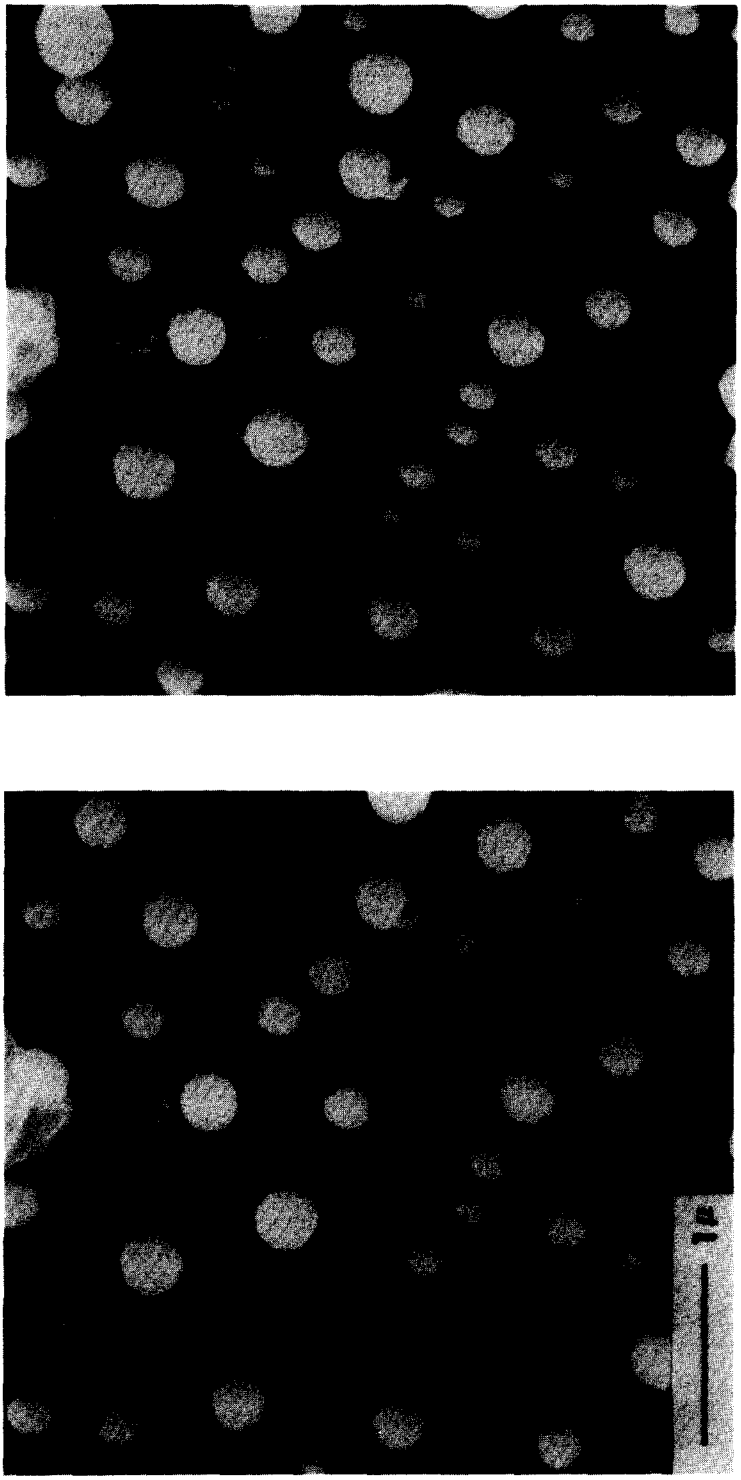

FIG. 3. SEM stereograph of air-annealed Pt/SiO$_2$ model catalyst (10 days, 1375 K, 5.3 Pa).

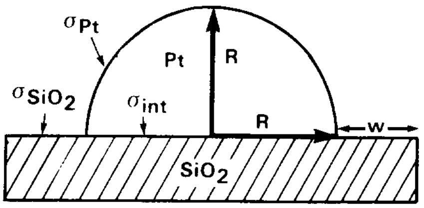

$$A_{Pt} = 2\pi R^2$$
$$A_{SiO_2} = 4\pi\left(R + \frac{w}{2}\right)\frac{w}{2}$$
$$A_{int} = \pi R^2$$

FIG. 4. The initial state of a Pt particle supported on a flat SiO_2 surface. The area of the SiO_2 surface is that of a flat ring of width w around the Pt particle.

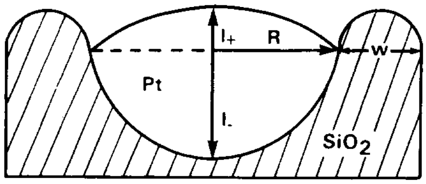

$$A_{Pt} = \pi(R^2 + l_+^2)$$
$$A_{SiO_2} = 2\pi^2\left(R + \frac{w}{2}\right)\left(\frac{w}{2}\right)$$
$$A_{int} = \pi(R^2 + l_-^2)$$

FIG. 5. The configuration of an encapsulated Pt particle on an SiO_2 surface.

each other and with the gas phase. The free energy of the system may be altered by changing the shape of the Pt particle and the SiO_2 surface in the manner shown in Fig. 5. The Pt hemisphere has become lenticular and is partially encapsulated in the SiO_2 surface while displaced SiO_2 forms a toroidal ridge around the perimeter of the Pt particle. This change, termed encapsulation, results in a decrease of the Pt surface area and in increases of both the SiO_2 surface and Pt–SiO_2 interfacial areas. The change in free energy associated with encapsulation is

$$\Delta F = \sigma_{Pt}\Delta A_{Pt} + \sigma_{SiO_2}\Delta A_{SiO_2} + \sigma_{int}\Delta A_{int}. \quad (2)$$

A driving force for encapsulation exists if $\Delta F < 0$. Since surface and interfacial energies are positive, the decrease in the energy of the system must come from a decrease in the area of the Pt surface. However, decreasing the Pt surface area may effect increases in the areas of the interface and the SiO_2 surface which oppose encapsulation. Given the values for σ_{Pt}, σ_{SiO_2}, and σ_{int}, ΔF may be calculated for the changing shape of the Pt particle and the SiO_2 support. The formula for the area of each surface and interface is shown in Fig. 5. The degree of encapsulation of the Pt particle is measured in terms of l_+, the height of the Pt surface above the SiO_2 plane, its value being R when the model is in the initial state (Fig. 4). With encapsulation, l_+ and the Pt surface area decrease. A_{int} may be calculated if the total volume of Pt is conserved. Under these conditions the volume of Pt equals $V_+ + V_-$, the volumes of the Pt above and below the SiO_2 plane. V_+ and V_- are obtained using the mensuration formula for a spherical segment,

$$V = \frac{\pi l}{6}(3R^2 + l^2).$$

In a similar manner A_{SiO_2} is obtained once the width of the toroidal ridge has been calculated. By setting the volume of the toroidal ridge equal to the volume of displaced SiO_2 which in turn equals V_-, the value of w can be obtained as a function of l_+. The volume of the toroidal ridge is

$$V_{ridge} = \pi^2\left(R + \frac{w}{2}\right)\left(\frac{w}{2}\right)^2.$$

The width of the ridge is also used to calculate A_{SiO_2} for the flat ring of SiO_2 in the initial state (Fig. 4).

Values for the surface energies of Pt and SiO_2 were taken from the literature; the surface energy of Pt at 1675 K is 2097 ± 50 erg cm^{-2} (*6*) and the surface energy of SiO_2 at 1575 K is 290 erg cm^{-2} (*8*). The Pt–SiO_2 interfacial energy has not been determined. Therefore, we used McLean's value for the Pt–Al_2O_3 interfacial energy at 1675 K, 1050 ± 80 erg cm^{-2} (*6*). The actual value of the Pt–SiO_2 interfacial energy may be higher than that of Pt–Al_2O_3 (*7*); however, it will be shown in a later section that while the magnitude of the interfacial energy does affect the degree of encapsulation, the effect is small over the range of probable values of the Pt–SiO_2 interfacial energy. Similarly, we assumed the temperature coefficient of the interfacial energy to be negligible since it is known that the coefficient is small for the surface energies of metals and oxides (*9*); the SiO_2 temperature coefficient is 0.03 erg cm^{-2} deg^{-1} (*8*).

The effect of encapsulation on the free energy of the model Pt/SiO_2 system as embodied in Eq. (2) is shown in Fig. 6 as a plot of $\Delta F/R^2$ versus l_+/R. Since the Pt particle radius R is held constant, R^2 behaves as a scaling factor for ΔF. The units for $\Delta F/R^2$ are ergs per square centimeter. The value of R in our SEM micrographs is 10^{-5} cm. The figure shows that encapsulation lowers the free energy of the model system. There is a minimum in the curve at $l_+ = 0.33\ R$. This minimum is the result of a constraint in the model, that R, the particle radius, be held constant. Thus, while this minimum does not represent a true equilibrium configuration, it does provide a qualitative description of the driving force for encapsulation which can be used to identify those factors which influence the mechanism of encapsulation. The configuration at $l_+ = 0.33\ R$ is shown in Fig. 5. There is striking similarity between the predicted configuration in Fig. 5 and the microstructures in Fig. 1d. The width of the ridge in Fig. 1d is ~30% of the diameter of the Pt particle, compared to 33% in Fig. 5.

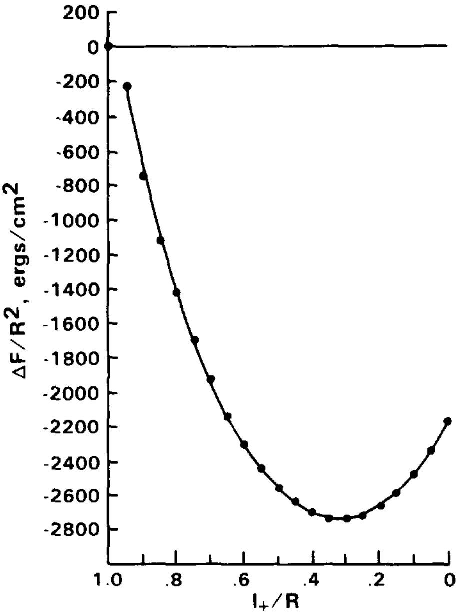

FIG. 6. Effect of encapsulation on free energy of Pt/SiO_2 system. R, the Pt particle radius, and R^2 are constants.

When $l_+ = 0.33\ R$, the reduction in free energy due to encapsulation is circa 17% of the energy of the initial state (Fig. 4). However, the energy reduction can be greater depending on the size of the SiO_2 ridge. The ridge is metastable and will decrease in size as SiO_2 diffuses across the SiO_2 surface away from the Pt particle. The presence of the ridge indicates that, under the conditions of these experiments, SiO_2 diffusion along the Pt–SiO_2 interface is faster than SiO_2 diffusion away from the ridge. If the conditions were such that the diffusion rates were reversed, the ridge would not form and the change in area of the SiO_2 with encapsulation would be small. This would further lower the free energy of the system to circa 22% of the energy of the initial state.

The Young–Dupre equation defines the contact angle θ that the Pt surface makes as it intersects the plane of the SiO_2 surface and the Pt–SiO_2 interface (*10*):

$$\sigma_{SiO_2} = \sigma_{int} + \sigma_{Pt} \cos \theta. \qquad (3)$$

The contact angle is measured between the Pt surface and the Pt–SiO_2 interface and is approximately 120° in Fig. 5. An angle of 111° is calculated using Eq. (3) and the same values of the Pt and SiO_2 surface energies and the Pt–SiO_2 interfacial energy used to obtain the configuration shown in Fig. 5. This configuration, then, is consistent with the requirements of the Young–Dupre equation.

Role of Surface and Interfacial Energy Values

The driving force for Pt encapsulation is the high surface energy of Pt relative to the Pt–SiO_2 interfacial energy. The role of the SiO_2 surface energy is contained in the transitory inhibition of encapsulation due to ridge formation. To evaluate the driving force for encapsulation we had to estimate the Pt–SiO_2 interfacial energy. The estimate we used, 1050 ± 80 ergs cm^{-2} (*6*), is smaller than has been observed in other metal–ceramic systems (*7*). The effect of the interfacial energy on the degree of encapsulation was determined by calculating the free energy change for several values of σ_{int} (Fig. 7). This figure shows that as the interfacial energy increases, the driving force and the apparent degree of encapsulation decrease. Even though the exact value of the interfacial energy is not known, Fig. 7 suggests that encapsulation may occur over a range of probable values for the interfacial energy.

Gas composition will also affect the driving force for encapsulation if it influences the surface and interfacial energies of the system. McLean and Mykura (*11*) showed that at 1375 K the surface energy of Pt decreased from 3120 erg cm^{-2} *in vacuo* to 2420 erg cm^{-2} in air. Assuming a temperature coefficient for Pt equal to −0.5 erg cm^{-2} deg^{-1} (*9*), the surface energy of Pt in air at 1675 K would be 2270 erg cm^{-2}. The surface energy of Pt used in our calculations was 2097 erg cm^{-2} (*6*), which predicted a free energy decrease of 17% at $l_+ = 0.33R$. Using 3120 erg cm^{-2} we would have predicted a greater free energy reduction: 25% at $l_+ = 0.25R$. Thus, a decrease in σ_{Pt} lowers the driving force for encapsulation, as in Eq. (2). Furthermore, since the surface energies of oxides are generally lower than those of the parent metals (*9*), temperature and atmosphere conditions which allow the formation of a surface layer of PtO_x will probably lower the driving force for encapsulation. If surface PtO_x formation occurs and we arbitrarily assume σ_{PtO_x} to be 1050 erg cm^{-2}, then for σ_{int} = 1050 erg cm^{-2} and σ_{SiO_2} = 290 erg cm^{-2}, the minimum free energy configuration occurs at $l_+ = 0.72R$, which is a reduction in the free energy of only 2%. Based on this model we would conclude that if Pt/SiO_2 catalysts are aged in air at temperatures at which PtO_x is stable and if the PtO_x surface energy is less than the Pt–SiO_2 interfacial energy, then encapsulation will not occur. When Pt/Al_2O_3 catalysts are oxygen annealed at 1025 K, Pt redispersion occurs due to the low surface energy of PtO_x which is formed under those conditions (*12*). Consequently, care must be taken to choose surface energies that are appropriate for the annealing environment. Since PtO_x is unstable under our experimental conditions (*11*), we used the surface energy of Pt metal.

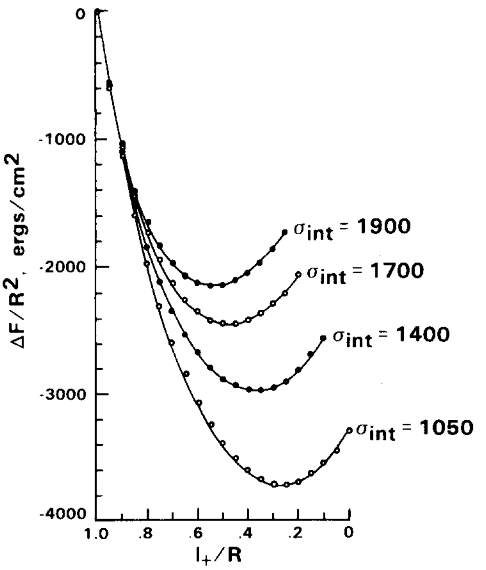

FIG. 7. Effect of magnitude of interfacial energy on the degree of encapsulation of Pt particles in the absence of ridge formation. *R*, the Pt particle radius, and R^2 are constants.

Discussion of the Model

This section contains a discussion of the assumptions used in constructing the model and the implications of encapsulation for aging phenomena of supported catalysts including particle growth.

The first assumption of the model was the definition of the free energy of the system. The definition as expressed by Eq. (1) applies to systems in which the Pt particle size is large. The relationship between particle size and thermodynamic properties is described by the Kelvin equation

$$\mu = \mu_0 + \frac{2\sigma\Omega}{R}, \tag{4}$$

where μ is the chemical potential of the component in a surface with a radius of curvature R, μ_0 is the chemical potential of the component in a flat surface, σ is the surface energy of that component, and Ω is the atomic or molecular volume of the component. Equation (4) indicates that as particle size decreases the chemical potential increases. When the Kelvin equation is incorporated into our definition of the free energy of the system, the free energy change of encapsulation is

$$\Delta F = \underbrace{\sigma_{\mathrm{Pt}}\Delta A_{\mathrm{Pt}} + \sigma_{\mathrm{int}}\Delta A_{\mathrm{int}} + \sigma_{\mathrm{SiO_2}}\Delta A_{\mathrm{SiO_2}}}_{\text{geometric area}} + \underbrace{\sum_i m_i\, 2\sigma_i\Omega_i\Delta \frac{1}{R_i}}_{\text{curvature}}, \tag{5}$$

where m_i is the number of atoms or molecules of the ith component in a surface whose radius of curvature is changing by an amount $\Delta 1/R_i$. For small R_i, the energy due to changes in the radius of curvature can be significant. Therefore, since one effect of encapsulation is to increase the radius of curvature of the Pt surface as shown in Fig. 5, encapsulation appears to be more favorable in small particle systems. However, Fig. 5 shows that encapsulation also decreases the radius of curvature at the Pt–SiO_2 interface, thus reducing the net driving force for encapsulation. Herring (*13*) has shown that for particles greater than 10 nm, the reduction in chemical potential with increasing size is negligible. Because the Pt particles observed in our study average 100 nm, we did not include the free energy contribution due to curvature in our calculations.

Ahn *et al.* (*14*) have shown that Pt particles supported on an undulated Al_2O_3 surface preferentially grow in the concave portions of the surface. Having shown that the radius of curvature of equivolume Pt particles increases as the particle moves from a convex surface to a concave surface, they attribute the preferred growth of Pt in concave sites to the lower chemical potential of the Pt in that configuration. They have applied their model to 4-nm Pt particles. However, since the experimental portion of Ahn's study deals with 100-nm particles, we feel that the free energy reduction associated with changing geometric surface area of the Pt/Al_2O_3 system is applicable in Ahn's study as well as in our studies of Pt/SiO_2 encapsulation. As noted above, the relevance of the Kelvin equation must not be overlooked for very small Pt particles.

Ahn's (*14*) study is particularly relevant to our studies of encapsulation because their SEM micrographs of aged Pt/Al_2O_3 samples also show evidence of encapsulation. The Pt particles in each trough or concave surface appear to be partially immersed in the Al_2O_3 surface. Furthermore, empty "depressions" much like those in Fig. 2 can be seen in Ahn's photomicrographs. Substituting surface energies and interfacial energy values for the Pt/Al_2O_3 system (*6*) into Eq. (2), our model predicts encapsulation with $l_+ = 0.25R$ (in the absence of ridge formation) with an energy reduction of 22% (Fig. 8). With ridge formation an energy reduction of 7% occurs at $l_+ = 0.45R$. As noted earlier, the minimum in the curve does not represent a true thermodynamic minimum, but does illustrate the

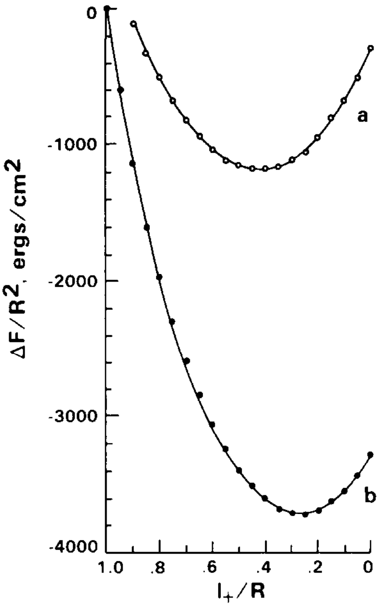

FIG. 8. Effect of encapsulation on the free energy of the Pt/Al_2O_3 system: (a) with Al_2O_3 ridge formation, (b) without ridge formation. R, the Pt particle radius, and R^2 are constants.

effect of ridge formation in the Pt/Al_2O_3 system.

The size of the Pt particles also influences the time necessary for encapsulation, since the size of a Pt particle determines the mass of SiO_2 that must be displaced. As the particle size decreases the diffusion distance and time (for SiO_2 transport out from under the Pt particle) also decrease. For example, if the diffusion distance decreases from 100 to 10 nm, the time required for diffusion decreases by two orders of magnitude (*15*). Consequently, encapsulation is more likely to be attained in small particle systems. Likewise, the disappearance of the ridge is also favored since the mass of the ridge is smaller. This latter effect suggests why ridges have not been reported before in electron microscope studies of supported Pt catalysts.

We also assumed that the Pt particle sinks into the SiO_2 surface, the displaced SiO_2 diffusing along the Pt–SiO_2 interface to the SiO_2 surface. Alternatively, SiO_2 diffusion up to and around the Pt particle could be a mechanism of encapsulation. The difference between these two mechanisms is that the latter requires SiO_2 surface diffusion up to and onto the Pt surface. Lund and Dumesic (*16*) have shown that when a Pt surface that has had SiO_2 deposited onto one half of it is annealed in air at 660 K, SiO_2 will diffuse and partially cover the previously SiO_2-free Pt surface. Whether SiO_2 diffuses along the Pt–SiO_2 interface or across the SiO_2 surface, Pt surface area is still reduced by converting it into Pt–SiO_2 interfacial area and therefore, the thermodynamic driving force for encapsulation, as defined in Eq. (2), remains the same.

Finally, our calculations have treated the Pt surface and Pt–SiO_2 interface as spherical segments. When we used formulae for ellipsoids instead of spherical segments, our model predicted the same driving force for encapsulation.

Encapsulation and Deactivation

The relationship between Pt encapsulation and catalyst deactivation is twofold. First, encapsulation is a form of catalyst deactivation since a decrease in the number of exposed Pt atoms occurs. The encapsulated particle in Fig. 5 has an exposed Pt area that is 45% lower than that of the hemispherical Pt particle in Fig. 4.

Second, encapsulation may also affect other deactivation processes. Ahn *et al.* (*14*) have noted that Pt particles in concave sites on Al_2O_3 are less likely to migrate out of those sites since this would result in an increase in the chemical potential of the particle. Similarly, migration of encapsulated particles would be inhibited since migration would increase the area of the exposed Pt. Consequently, particle growth of encapsulated Pt would probably occur by interparticle diffusion of Pt atoms or PtO_x molecules. However, the growth of an encapsulated particle would require that either (1) the growing Pt particle bulge out of its "depression" which is thermodynamically unfavored, or (2) the depression enlarge to accommodate the larger Pt particle, a kinetically inhibited process. Thus encapsulation may inhibit both mechanisms of particle growth.

CONCLUSIONS

If the surface energy of a Pt particle is greater than the interfacial energy of the Pt and the SiO_2 or Al_2O_3 support, then a thermodynamic driving force exists for partial encapsulation of the Pt particle. Under some conditions encapsulation causes the formation of a toroidal ridge around the base of the Pt particle and this ridge can be observed with a scanning electron microscope.

Encapsulation lowers the area of exposed Pt surface and may be a form of catalyst deactivation. As such, this mechanism is previously unreported. This model of the encapsulation process can be applied to other supported catalyst systems if the appropriate surface and interfacial energies are known. Finally, encapsulation may inhibit the particle growth.

ACKNOWLEDGMENTS

The authors thank Mr. Walt Lange for SEM characterization of the samples and Dr. David Eddy for the use of his high temperature furnaces. The authors especially acknowledge Mr. Glenn Sutherland for his technical advice on the science and art of sputtering.

REFERENCES

1. Ruckenstein, E., and Pulvermacher, B., *J. Catal.* **29,** 224 (1973).
2. Wynblatt, P., Dalla Betta, R. A., and Gjostein, N. A., *in* "The Physical Basis for Heterogeneous Catalysis" (E. Drauglis and R. I. Jaffee, Eds.), p. 501. Plenum, New York, 1975.
3. Flynn, P. C., and Wanke, S. E., *J. Catal.* **34,** 390 (1974).
4. Baker, R. T. K., Thomas, C., and Thomas, R. B., *J. Catal.* **38,** 510 (1975).
5. Chen, M., and Schmidt, L. D., *J. Catal.* **55,** 348 (1978).
6. McLean, M., and Hondros, E. D., *J. Mater. Sci.* **6,** 19 (1971).
7. Hondros, E. D., *in* "Proceedings of the Conference on Interfaces," p. 77. Butterworths, London, 1970.
8. Kingery, W. D., *J. Amer. Ceram. Soc.* **42,** 6 (1959).
9. Overbury, S. H., Bertrand, P. A., and Somorjai, G. A., *Chem. Rev.* **75,** 547 (1975).
10. Adamson, A. W., "Physical Chemistry of Surfaces," 1st ed., p. 265. Interscience, New York, 1962.
11. McLean, M., and Mykura, N., *Surf. Sci.* **5,** 466 (1966).
12. Ruckenstein, E., and Chu, Y. F., *J. Catal.* **59,** 109 (1979).
13. Herring, C., "Structure and Properties of Solid Surfaces," p. 5. Univ. of Chicago Press, Chicago, 1953.
14. Ahn, T., Tien, J. K., and Wynblatt, P., *J. Catal.* **66,** 335 (1980).
15. Kingery, W. D., "Introduction to Ceramics," 1st ed., p. 222. Wiley, New York, 1960.
16. Lund, C. R. F., and Dumesic, J. A., *J. Catal.* **72,** 21 (1981).